

Time Series Transformer-Based Modeling of Pavement Skid and Texture Deterioration

Lu Gao, Ph.D.¹, Zia Ud Din, Ph.D.¹, Kinam Kim, Ph.D.¹, and Ahmed Senouci, Ph.D.¹

¹Department of Civil and Environmental Engineering, University of Houston

Abstract

This study investigates the deterioration of skid resistance and surface macrotexture following preventive maintenance using micro-milling techniques. Field data were collected from 31 asphalt pavement sections located across four climatic zones in Texas. The data encompasses a variety of surface types, milling depths, operational speeds, and drum configurations. A standardized data collection protocol was followed, with measurements taken before milling, immediately after treatment, and at 3, 6, 12, and 18 months post-treatment. Skid number and Mean Profile Depth (MPD) were used to evaluate surface friction and texture characteristics. The dataset was reformatted into a time-series structure with 930 observations, including contextual variables such as climatic zone, treatment parameters, and baseline surface condition. A comparative modeling framework was applied to predict the deterioration trends of both skid resistance and macrotexture over time. Eight regression models, including linear, tree-based, and ensemble methods, were evaluated alongside a time series transformer model. Results show that the transformer model achieved the highest prediction accuracy for skid resistance ($R^2 = 0.981$), while Random Forest performing best for macrotexture prediction ($R^2 = 0.838$). The findings indicate that the degradation of surface characteristics after preventive maintenance is nonlinear and influenced by a combination of environmental and operational factors. This study demonstrates the effectiveness of data-driven modeling in supporting transportation agencies with pavement performance forecasting and maintenance planning.

Keywords: Pavement deterioration, skid resistance, pavement performance modeling, transformer, time series, macrotexture, micro-milling, machine learning, deep learning, preventive maintenance

1 Introduction

Pavement surface characteristics such as skid resistance and macrotexture are crucial indicators for ensuring road safety and preventing accidents [1]. Skid resistance, the friction generated between tires and the pavement surface, is fundamental for vehicle control during critical maneuvers like turning and emergency braking [2]. A significant decrease in skid resistance can lead to a considerable increase in accident rates, and higher skid numbers are consistently associated with fewer crashes [3]. Macrotexture, defined as the surface texture component with wavelengths between 0.5 and 50 mm, plays a vital role in removing water film from the tire-pavement contact area and contributes to skid resistance, particularly at higher speeds and in wet conditions [4]. Both microtexture (roughness less than 0.5 mm) and macrotexture together determine the overall pavement friction. Pavement skid resistance undergoes a natural progression of change over time due to traffic and environmental influences. It may initially increase as the asphalt binder wears away, then decline as the aggregate becomes polished, and eventually reach a stable state [5]. Therefore, consistent monitoring and maintenance of these pavement surface characteristics are essential to maintain adequate traction and mitigate crash risks, especially under wet weather conditions [6].

Preventive maintenance techniques, such as micro-surfacing and milling operations, are applied to significantly alter existing pavement surface properties [7]. For instance, micro-surfacing aims to improve anti-skid performance, wear resistance, and durability. It also addresses noise reduction through optimized gradation and the inclusion of additives like rubber powder and fiber [8]. However, the effectiveness of such treatments remains insufficiently quantified. This study addresses the following research question: How do skid resistance and surface macrotexture deteriorate over time after micro-milling treatments; and to what extent can sequence-based machine learning models improve the prediction of this degradation compared to traditional approaches?

2 Literature Review

2.1 The impact of skid resistance and surface texture on road safety

Pavement skid resistance is a critical factor for ensuring road safety and preventing accidents [9]. Insufficient skid resistance is identified as a significant cause of road traffic crashes, accounting for approximately 30% of such incidents worldwide annually [1]. While newly constructed pavements generally exhibit high skid resistance, this property continuously deteriorates over time due to the repeated actions of traffic loads and environmental factors [10]. For asphalt pavements, the

deterioration typically follows a pattern: an initial increase in friction as the asphalt binder is stripped, followed by a decline as the aggregate surface polishes, and finally stabilizes in the late period [11].

The ability of a pavement to resist skidding is heavily influenced by its surface texture, which is categorized into micro-texture and macro-texture [2]. Micro-texture refers to the fine-scale roughness of the aggregate surface, with wavelengths less than 0.5 mm, and primarily contributes to adhesion and friction at low speeds [12]. Macro-texture, on the other hand, involves larger irregularities with wavelengths between 0.5 mm and 50 mm, which are crucial for hysteretic phenomena, effective water drainage, and maintaining skid resistance at higher speeds [13]. The presence of water or other contaminants on the pavement surface complicates the role of texture by reducing the tire-pavement contact area and building up hydrodynamic pressure, thereby increasing the risk of skidding and hydroplaning [14].

A strong correlation exists between pavement surface friction values and road safety. Higher skid resistance usually linked to reduced crash frequencies, particularly under wet conditions [3]. Studies have shown that a 10-unit increase in Skid Number (SN) can lead to a 7% to 8% reduction in dry-weather crashes and a more significant 14% to 21% decrease in wet-weather crashes on highways [15]. The impact of increased skid resistance is especially pronounced on interstate highways and curved segments during wet conditions, where friction demand is higher [16].

2.2 Influence of micro-milling treatment on skid resistance and surface texture

Micro-milling is a cost-effective pavement preservation technique widely adopted in highway maintenance and rehabilitation [17]. This method involves removing a thin layer of existing asphalt pavement, typically as little as 3/8 inch (9.5 mm) or 1.5–2 cm for tunnel concrete pavement, using a cutting drum equipped with numerous small, tightly-spaced teeth [18]. The primary goals of micro-milling include improving skid resistance, restoring the road's profile, and removing surface distresses such as raveling or minor rutting before applying a new overlay. The micro-milled surface can be opened directly to traffic, giving contractors greater flexibility [19].

The effectiveness of micro-milling on surface texture and skid resistance is significantly influenced by operational factors. Sections milled with fine drums, typical of micro-milling, demonstrate enhanced skid resistance and macrotexture [7]. Higher forward milling speeds also correlate positively with improved skid resistance and macrotexture. The recommended speeds ranges from 70 to 80 feet per minute [18]. Optimal cutting depths for texturing are typically between 0.25 and

0.5 inches (6 to 13 mm). However, the milling depth itself does not notably impact the long-term deterioration of skid resistance or macrotexture [20].

Micro-milling faces challenges in achieving consistent texture and depth. Factors such as existing pavement distress, machine performance, and drum rotation rates can influence these outcomes [21]. Inconsistent milling can compromise bonding strength, leading to premature distress such as peeling or shoving in the overlay [22]. Micro-milling has demonstrated service lives ranging from about 12 months on seal coats to 10-12 years on hot-mix asphalt (HMA) sections [23].

2.3 Factors affecting skid resistance and surface texture deterioration

Pavement skid resistance is not static. It continuously deteriorates over time due to various influencing factors, primarily traffic loads and environmental conditions [24]. The deterioration process usually occurs in stages: first, a rapid increase due to binder removal, then a slow decrease as aggregate micro-texture worsens, and finally, a stabilization phase [25]. Vehicular traffic, through its polishing effect, is a major contributor to this decline, especially in the wheel path areas [26]. Vehicle movement determines the direction of polishing. Acceleration-dominated areas face higher friction against traffic flow, while deceleration-dominated areas experience lower friction in the direction of traffic flow [27]. Environmental factors, including water, snow, ice, and contaminants like rubber deposits, significantly reduce skid resistance. They do this by forming a lubricating film or covering the surface texture [28]. Water film thickness, in particular, negatively correlates with skid resistance and can lead to hydroplaning at higher speeds. Temperature (both tire and ambient/pavement) can also influence skid resistance, with increases often leading to a reduction [29].

Beyond traffic and environmental effects, specific material and design choices, such as the use of composite aggregates, significantly impact skid resistance and its long-term performance [30, 31]. The mineralogy of aggregates greatly influences their susceptibility to wear and polishing. For example, poly-mineral aggregates tend to exhibit higher polishing resistance and friction than mono-mineral ones like limestone [32]. Aggregate dimension also plays a role, with finer aggregates typically providing higher initial friction but experiencing a more pronounced reduction with polishing [33]. For asphalt mixtures, the long-term skid resistance is primarily determined by coarse aggregates, while fine aggregates mainly affect the initial friction [34].

The type and dosage of binder can influence the initial stripping phase, which affects both friction values and the time required for complete binder removal [35]. Pavement macro-texture and

air voids are crucial, as they influence the actual tire-pavement contact area and drainage capacity [36]. The use of recycled materials like reclaimed asphalt pavement (RAP) or crumb rubber, and warm mix asphalt (WMA) additives, may have a detrimental effect on skid resistance and can delay binder removal [37]. Grooving pavements improves drainage and skid resistance, and reduces hydroplaning risk. However, groove deterioration from wear or rubber deposits can lessen their effectiveness [38]. Pavement markings also influence skid resistance. The materials used and glass beads can decrease friction compared to the surrounding pavement. However, anti-skid additives can help to reduce this effect. [39].

2.4 Deterioration modeling of skid Resistance and surface texture

Modeling pavement skid resistance and texture deterioration is vital for road safety and maintenance. It helps understand the complex interactions between vehicle tires and road surfaces [40]. Various analytical, statistical, and machine learning models have been developed to predict and understand these time-dependent properties [41–43].

Statistical and analytical models have traditionally been used to describe the decay of pavement conditions [44–46]. Common approaches include empirical relationships and regression models. These link pavement characteristics to skid resistance or its decline rate. Characteristics used include texture parameters like Mean Texture Depth (MTD) and Mean Profile Depth (MPD) [47]. Models like the Penn State model, PIARC International Friction Index (IFI), and the Rose and Gallaway model are examples that estimate skid resistance as a function of speed and texture, though they often have limitations regarding water film thickness or application scope [48]. Skid resistance often declines rapidly at first, then slows, eventually stabilizing. Models like asymptotic, exponential, and logarithmic ones capture this behavior [49]. However, these statistical methods may struggle with non-linear relationships and the multitude of influencing factors, leading to limited accuracy and applicability [50].

Machine learning (ML) has emerged as a powerful tool for predicting pavement conditions. It overcomes the limitations of traditional statistical models by handling complex, non-linear relationships and multi-dimensional data [51–55]. Widely applied ML algorithms include Artificial Neural Networks (ANN), Support Vector Machines (SVM), Random Forest (RF), and Decision Trees (DT) [51]. These models leverage various input parameters, such as vehicle speed, water depth, tire tread depth, pavement macro-texture, aggregate properties, and even environmental factors, to predict friction coefficients or classify skid resistance levels (e.g., low, medium, high) [56].

Data from 3D laser scanning and other non-contact measurement methods provide high-resolution texture information as input for these ML models, improving prediction accuracy [10].

More advanced AI and ensemble learning models are continually being developed to enhance prediction accuracy and interpretability [53, 57]. Neural networks optimized by genetic algorithms demonstrate strong self-learning capabilities. They can establish highly non-linear relationships for skid resistance prediction. This applies even to long-term analysis and specific pavement types, such as steel bridge deck pavement [58]. Light Gradient Boosting Machine (LightGBM) and its optimized variant, Bayesian-LightGBM, are known for their stability, generalization, and efficiency in multi-factor regression. They significantly improve prediction accuracy over other models [47].

Deep learning approaches, such as Convolutional Neural Networks (CNN) and deep residual networks (ResNets), are also being explored, particularly with 3D texture data, to achieve higher accuracy in correlating texture with friction [10, 59]. Integrated frameworks that combine techniques such as Fast Fourier Transform (FFT) with Extreme Gradient Boosting (XGBoost) or wavelet transforms with fractal theory enhance texture characterization and improve skid resistance prediction. These frameworks provide insights into the impact of multi-scale texture features [60].

2.5 Limitations and Research Gaps

While several studies have investigated the degradation of pavement skid resistance and surface texture, important limitations remain, especially in the context of their evolution after preventive maintenance treatments. Most existing models rely on traditional statistical or machine learning approaches that treat each data point as independent. As a result, they fail to consider the temporal continuity and dynamic progression of surface performance over time. These approaches often overlook how previous surface conditions and operational factors influence future outcomes, leading to reduced predictive accuracy in long-term assessments. There is a clear need for models that can capture time-dependent patterns and complex relationships among treatment parameters, environmental conditions, and surface characteristics. This study addresses this gap by proposing a sequence-based Transformer model that treats the degradation of skid resistance and texture after maintenance as a temporal learning problem.

3 Methodology

3.1 Problem Formulation

Predicting the temporal evolution of pavement skid resistance is a classic sequence-to-one time series regression task. In this task, the model uses a sequence of past pavement conditions to predict what the road will be like at the next inspection. For example, if the past five years of data are available, the model learns patterns from those five years and uses them to forecast the skid resistance and texture for the sixth year. For a given test section, a finite sequence of feature vectors $\mathbf{x}_0, \mathbf{x}_1, \dots, \mathbf{x}_T$ is observed at discrete time points t_0, t_1, \dots, t_T , where each $\mathbf{x}_t \in \mathbb{R}^{d_x}$ represents the concatenation of all feature values observed at time t . Given a sliding window of length L , the Transformer receives the ordered sequence

$$\mathbf{X}_{t-L+1:t} = \begin{bmatrix} \mathbf{x}_{t-L+1} \\ \vdots \\ \mathbf{x}_t \end{bmatrix} \in \mathbb{R}^{L \times d_x} \quad (1)$$

as input and outputs a forecast $\hat{y}_{t+\Delta t} \in \mathbb{R}$ of the skid number at the next inspection point $t + \Delta t$.

To capture both short- and long-term temporal dependencies in this sequence-to-one prediction task, the Transformer model [61] was adopted. Its self-attention mechanism makes it well-suited for time series forecasting, especially when handling long-range dependencies and multivariate inputs.

3.2 Time Series Transformer

The Transformer architecture, originally developed for natural language processing, is well suited for time series forecasting tasks with complex temporal dependencies. Unlike traditional models such as ARIMA or recurrent neural networks (RNNs), which process sequences sequentially, the transformer utilizes a self-attention mechanism that considers all time steps simultaneously. This enables the model to more effectively capture long-range dependencies and interactions among variables across time [62].

Time Series transformers adapt the original transformer architecture to forecasting problems by replacing word embeddings with time series feature vectors and modifying the positional encoding to reflect temporal structure. These models are capable of handling multivariate inputs, irregular time steps, and long input sequences. Time series transformers have been widely applied in multivariate forecasting tasks [63–65]. The following section introduces the key concepts of the Transformer architecture.

3.2.1 Feature Embedding and Positional Encoding

The Transformer is a neural architecture designed for sequence modeling. The Transformer architecture processes all inputs within a common latent space of fixed dimensionality d_{model} . This design allows the model to uniformly apply self-attention and feed-forward layers regardless of the input's original structure or scale. To accommodate this, each input vector $\mathbf{x}_t \in \mathbb{R}^{d_x}$ is first projected into the latent space through a learned linear transformation [61]:

$$\mathbf{h}_t^{(0)} = \mathbf{E} \mathbf{x}_t, \quad \mathbf{E} \in \mathbb{R}^{d_{\text{model}} \times d_x}. \quad (2)$$

The resulting vector $\mathbf{h}_t^{(0)}$ serves as the initial token representation for time t , prior to any self-attention processing.

To retain the temporal order of the sequence, a positional encoding vector $\mathbf{p}_t \in \mathbb{R}^{d_{\text{model}}}$ is added to each embedding. This positional signal distinguishes tokens from different time steps, even if their feature content is similar. A widely used deterministic choice is the sinusoidal encoding [61]:

$$(\mathbf{p}_t)_{2k} = \sin\left(\frac{t}{10000^{2k/d_{\text{model}}}}\right), \quad (\mathbf{p}_t)_{2k+1} = \cos\left(\frac{t}{10000^{2k/d_{\text{model}}}}\right), \quad (3)$$

for $k = 0, \dots, \lfloor d_{\text{model}}/2 \rfloor - 1$. This scheme encodes different frequencies along dimensions of the embedding, allowing the model to represent both coarse and fine temporal patterns. The final input to the encoder is a sequence of order-aware embeddings formed by addition:

$$\tilde{\mathbf{h}}_t^{(0)} = \mathbf{h}_t^{(0)} + \mathbf{p}_t, \quad \mathbf{H}^{(0)} = [\tilde{\mathbf{h}}_{t-L+1}^{(0)}, \dots, \tilde{\mathbf{h}}_t^{(0)}] \in \mathbb{R}^{L \times d_{\text{model}}} \quad (4)$$

The addition (rather than concatenation) ensures that the input dimensionality to the encoder remains fixed at d_{model} .

3.2.2 Self-Attention Encoder

Each Transformer encoder layer consists of two main components: multi-head self-attention, which allows the model to relate each time step to every other time step in the input sequence, and a position-wise feed-forward network (FFN), which processes each time step independently through a small neural network to enhance the model's capacity. To make training more stable and efficient, the Transformer adds the original input back to the output of each part (a technique called a residual connection) and then applies a method called layer normalization, which adjusts the values to be more balanced and consistent. These techniques help the model learn better and avoid problems like exploding or vanishing gradients.

Let $\mathbf{H}^{(l)} \in \mathbb{R}^{L \times d_{\text{model}}}$ be the input to layer l . Following the scaled-dot attention of Vaswani et al. [61], the self-attention mechanism computes query, key, and value matrices:

$$\mathbf{Q} = \mathbf{H}^{(l)} \mathbf{W}_Q, \quad \mathbf{K} = \mathbf{H}^{(l)} \mathbf{W}_K, \quad \mathbf{V} = \mathbf{H}^{(l)} \mathbf{W}_V, \quad (5)$$

where $\mathbf{W}_Q, \mathbf{W}_K, \mathbf{W}_V \in \mathbb{R}^{d_{\text{model}} \times d_k}$ are learned parameters. Attention weights are computed via scaled dot-product:

$$\mathbf{A} = \text{softmax} \left(\frac{\mathbf{Q}\mathbf{K}^\top}{\sqrt{d_k}} \right) \in \mathbb{R}^{L \times L}, \quad (6)$$

and the attention output is

$$\text{Attn}(\mathbf{Q}, \mathbf{K}, \mathbf{V}) = \mathbf{A}\mathbf{V} \in \mathbb{R}^{L \times d_k}. \quad (7)$$

Using H independent attention heads allows the model to capture diverse interaction patterns. Their outputs are concatenated and linearly projected back [61]:

$$\text{MHA}^{(l)}(\mathbf{H}^{(l)}) = \left[\text{Attn}^{(1)} \parallel \dots \parallel \text{Attn}^{(H)} \right] \mathbf{W}_O, \quad (8)$$

with $\mathbf{W}_O \in \mathbb{R}^{Hd_k \times d_{\text{model}}}$.

Each sub-layer includes a residual connection and layer normalization:

$$\tilde{\mathbf{H}}^{(l)} = \text{LayerNorm} \left(\mathbf{H}^{(l)} + \text{MHA}^{(l)}(\mathbf{H}^{(l)}) \right). \quad (9)$$

Following Vaswani et al. [61], a feed-forward network is then applied to each time step independently:

$$\text{FFN}(\mathbf{h}) = \sigma(\mathbf{h}\mathbf{W}_1 + \mathbf{b}_1)\mathbf{W}_2 + \mathbf{b}_2, \quad (10)$$

Using residual connections [66] and layer normalization [67], the final output of the encoder layer is:

$$\mathbf{H}^{(l+1)} = \text{LayerNorm} \left(\tilde{\mathbf{H}}^{(l)} + \text{FFN}(\tilde{\mathbf{H}}^{(l)}) \right). \quad (11)$$

Stacking N such layers yields the final output $\mathbf{H}^{(N)}$, which captures contextual information from the entire input sequence.

3.2.3 Sequence Pooling and Regression Head

Following common practice in Transformer-based regression models (e.g., Vaswani et al. [61]), the final time-step embedding $\mathbf{h}_t^{(N)}$ is extracted and passed through a small multi-layer perceptron.

$$\hat{y}_{t+\Delta t} = \mathbf{w}_2^\top \sigma(\mathbf{W}_1 \mathbf{h}_t^{(N)} + \mathbf{b}_1) + b_2. \quad (12)$$

3.3 Loss Function and Optimisation

The network parameters Θ are trained to minimise the mean-squared error, commonly used in regression tasks [68].

$$\mathcal{L}(\Theta) = \frac{1}{N} \sum_{i=1}^N (y_i - \hat{y}_i)^2, \quad (13)$$

where N is the number of (sequence, target) pairs in the training set. Stochastic gradient descent with adaptive learning rate is typically used, coupled with early stopping on a validation set.

4 Case Study

4.1 Data Collection

The data used in this study were obtained from a research initiative conducted by the Texas Department of Transportation (TxDOT) to evaluate the short-term effectiveness of micro-milling in improving pavement skid resistance. The study involved 31 pavement sections across multiple regions of Texas, with repeated measurements collected over time to monitor changes in surface conditions. The selected test sections span multiple climatic zones across the state of Texas (Figure 1). These sections are distributed across various TxDOT districts, including San Angelo, San Antonio, Abilene, and Tyler. In total, the study includes 16 seal coat sections and 15 HMA sections located on major roadways such as US 87, SH 151, US 277, I-20 West, and Wurzbach Parkway.

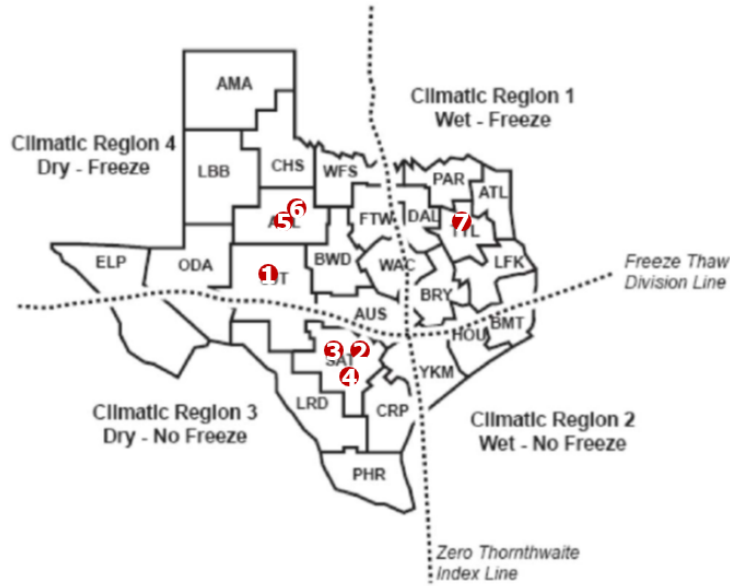


Figure 1: Test Sits

Note: 1. US 87 (SJT); 2. Wurzbach Parkway (SAT); 3. SH 151-1 (SAT); 4. SH 151-2 (SAT); 5. US 277-1 (ABL); 6. US 277-2 (ABL); 7. I-20 (TYL)

Figures 2a to 2e illustrate the layouts of selected experiment sections across several highway corridors in Texas. These layouts represent a subset of the full set of test segments used in this study, chosen to highlight typical field configurations and treatment variations. Figure 2a shows the configuration of a test site along US87, where uniformly spaced short segments were prepared to investigate short-term changes under consistent baseline conditions. This site enabled detailed tracking of texture and friction immediately after milling. The Wurzbach Parkway layout, shown in Figure 2b, includes longer segments with varying milling speeds and depths, designed to capture the influence of operational parameters on surface evolution. Figure 2c illustrates another configuration on SH151. Two sets of experimental sections along US277 are depicted in Figures 2d and 2e. These segments span a broader range of milling depths and were constructed during two separate phases.

Beyond segment configurations, Figure 2 also emphasizes the geographic and contextual diversity of the experiment sites. The five locations span urban and rural corridors, including major highways and regional roads across different TxDOT districts. This geographic spread allows the study to capture a broader range of traffic loading conditions, construction practices, and environmental exposures—factors that significantly influence surface deterioration. By including sites such as Wurzbach Parkway in a metropolitan area and US277 in rural regions, the dataset used in this case

study supports more generalizable modeling and enables performance comparisons across varying climatic zones, pavement types, and maintenance practices.

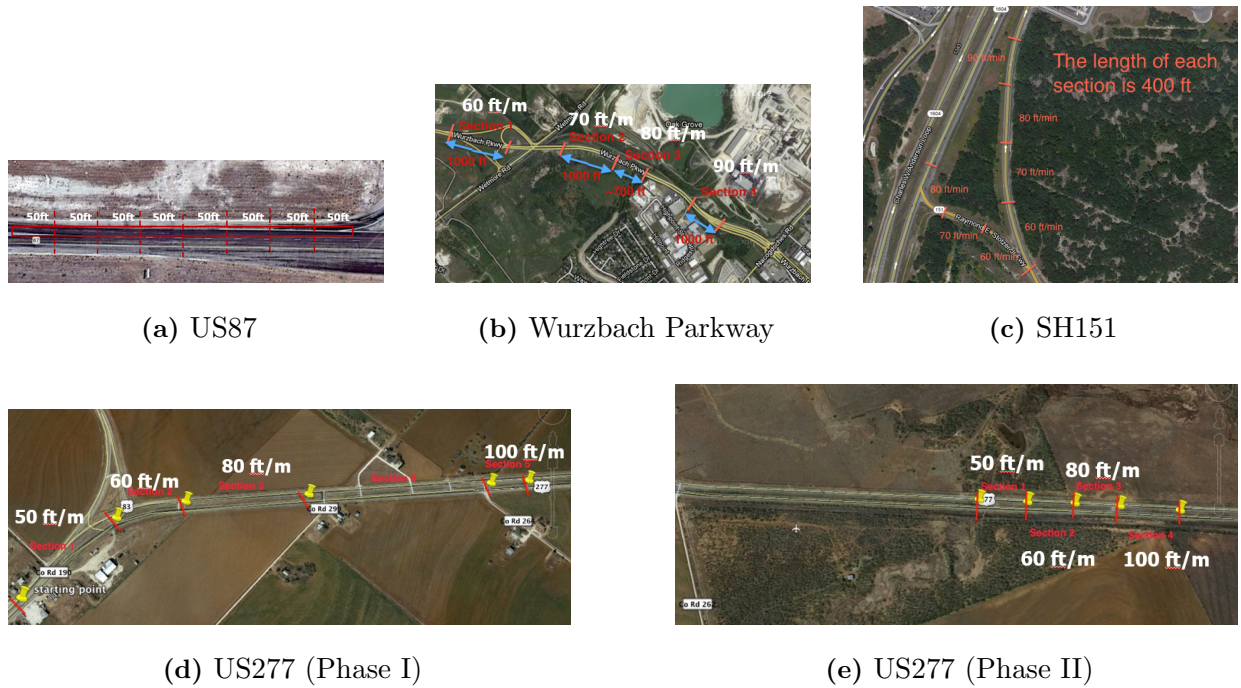


Figure 2: Experiment section layouts at five locations

To improve surface texture and skid resistance, surface treatments were applied using either standard milling drums with approximately 150 teeth or fine-milling drums with around 300 teeth. Milling depths ranged from 0.2 to 0.5 inches, and machine operating speeds varied between 30 and 100 feet per minute. Each pavement section underwent a controlled surface texturing treatment, during which engineers recorded key operational parameters such as milling depth, drum type, and machine speed. Representative field photos of the roadway before treatment and the milling process in operation are shown in Figure 3, which illustrates key stages of the micro-milling process. Figure 3a shows the pavement surface prior to treatment. Visually, the surface appears uniformly dark and smooth, with a noticeable sheen caused by aggregate polishing over time. This shiny black coloration is a common indicator of severely reduced macrotexture and microtexture, which suggests low skid resistance. Such conditions can significantly impair tire-pavement friction, especially in wet weather, and increase crash risks. Figure 3b illustrates the micro-milling process, during which the worn and polished surface layer is removed to restore surface texture. This operation exposes a rougher, lighter-colored aggregate matrix, which improves macrotexture and enhances skid resistance.



(a) Roadway before milling operation



(b) Milling machinery in operation

Figure 3: Milling Operation on Roadway

Following treatment, each section was monitored at six scheduled time points: a baseline measurement before treatment, and follow-up measurements at approximately 0, 3, 6, 12, and 18 months after treatment. Figure 4 displays the pavement surface before, immediately after, and three months following micro-milling at three chosen sites. At every time point, three replicate measurements were taken across the left, center, and right wheel paths of each lane to ensure spatial representativeness and data reliability.

The pre-treatment surfaces at US87 (Figure 4a), Wurzbach Parkway (Figure 4d), and SH151 (Figure 4g) exhibit varying degrees of aggregate polishing and binder flushing. In particular, the US87 section demonstrates a noticeably darker and smoother surface, indicative of low friction due to binder bleeding and reduced macrotexture. The Wurzbach and SH151 sections show moderately exposed aggregates; however, the presence of surface fines suggests macrotexture infill and diminished surface drainage capability.

Immediately after treatment, the images reveal a substantial improvement in surface texture uniformity and roughness. For instance, the US87 section (Figure 4b) displays an open-textured and lighter-colored surface, which indicates successful removal of the oxidized top layer. The Wurzbach Parkway and SH151 sections (Figures 4e and 4h) exhibit well-defined milling grooves and consistent texturing, reflective of a uniform cutting depth across the lane width. The increased surface roughness at this stage aligns with the immediate post-treatment rise in skid resistance observed in field data.

At three months post-treatment, changes in surface condition begin to emerge. The US87 section (Figure 4c) shows evidence of re-polishing, with aggregate edges becoming less distinct, which suggests early-stage wear-in under traffic loading. In contrast, the textures at Wurzbach Parkway

and SH151 (Figures 4f and 4i) remain relatively well-preserved, with groove patterns still clearly visible. This difference may be attributed to variations in traffic volume, aggregate hardness, or binder type.



Figure 4: Pavement surfaces before, after, and 3 months after milling at three selected locations

During each monitoring event, several variables were recorded. Skid resistance was assessed using both a locked-wheel skid trailer and a British Pendulum Tester. Surface texture was evaluated through the Sand Patch Test, Circular Texture Meter (CTM), and 3D laser scanning, yielding indicators such as Mean Profile Depth (MPD). Operational parameters, including milling depth, drum configuration, and machine speed, were also documented.

4.2 Data Description

The final dataset comprises 324 samples, each representing a specific lane segment at a particular time point during the monitoring period. These samples were collected from multiple pavement sections located in different climatic regions across Texas. The dataset incorporates a wide range of information, including skid resistance measurements, surface texture indicators, environmental conditions, and operational parameters from the surface treatment process, such as milling depth and machine speed. Table 1 provides descriptive statistics and variable definitions for all selected features included in the analysis. Continuous variables such as skid number and macrotexture depth exhibit substantial variability. For example, the measured skid number ranges from as low as 10.5 to as high as 47.0 across different time points, while macrotexture depth after milling spans from 0.48 to 3.58 mm. Categorical variables were encoded numerically to support machine learning workflows. For instance, surface type is coded as 0 for HMA and 1 for seal coat, while climatic zone is simplified into two categories: dry-freeze (0) and dry-non-freeze (1), based on available data. Similarly, drum type is represented as 0 for fine milling drums (300 teeth) and 1 for standard drums (150 teeth).

Table 1: Descriptions and summary statistics for all selected variables

Variable	Description / Encoding	Mean	Std. Dev.	Min	Max
Climatic Zone	0 = dry-freeze, 1 = dry-non-freeze	0.40	0.49	0	1
Depth (In)	Milling depth in inches	0.46	0.11	0.20	0.50
Drum	0 = Fine drum (300 teeth), 1 = Standard drum (150 teeth)	0.70	0.46	0	1
Macrotexture (mm)	Measured texture depth	1.44	0.69	0.28	2.89
Macrotexture after milling (mm)	Texture depth after milling	2.37	0.59	0.48	3.58
Macrotexture before milling (mm)	Texture depth before milling	0.68	0.32	0.16	1.73
Month	Months since treatment (0 = base-line)	9.75	5.77	3.00	18.00
Skid Number	Friction measure at given month	29.91	9.59	10.50	47.00
Skid Number after milling	Friction measure immediately after milling	42.37	12.15	15.00	58.00
Skid Number before milling	Friction measure before milling	15.70	8.00	9.00	35.00
Speed (fpm)	Milling machine speed (ft/min)	68.52	17.81	30.00	100.00
Surface Type	0 = HMA, 1 = Seal Coat	0.59	0.50	0	1

Figure 5 shows the distribution of all selected variables used in the modeling process. The skid number before milling is heavily left-skewed, which indicates that most segments started with relatively low friction levels. In contrast, skid number after milling shifts to higher values, which demonstrates the immediate effectiveness of surface treatment in improving friction. The skid number measured over time displays a more balanced distribution, capturing the degradation trend across months. The month variable itself shows a discrete distribution corresponding to scheduled inspection intervals (3, 6, 12, and 18 months). Categorical variables such as drum type, climatic zone, and surface type were encoded numerically and appear as bimodal distributions. These reflect the study design, where standard and fine drums, dry-freeze and dry-non-freeze regions, and HMA versus seal coat surfaces were all included in roughly balanced proportions.

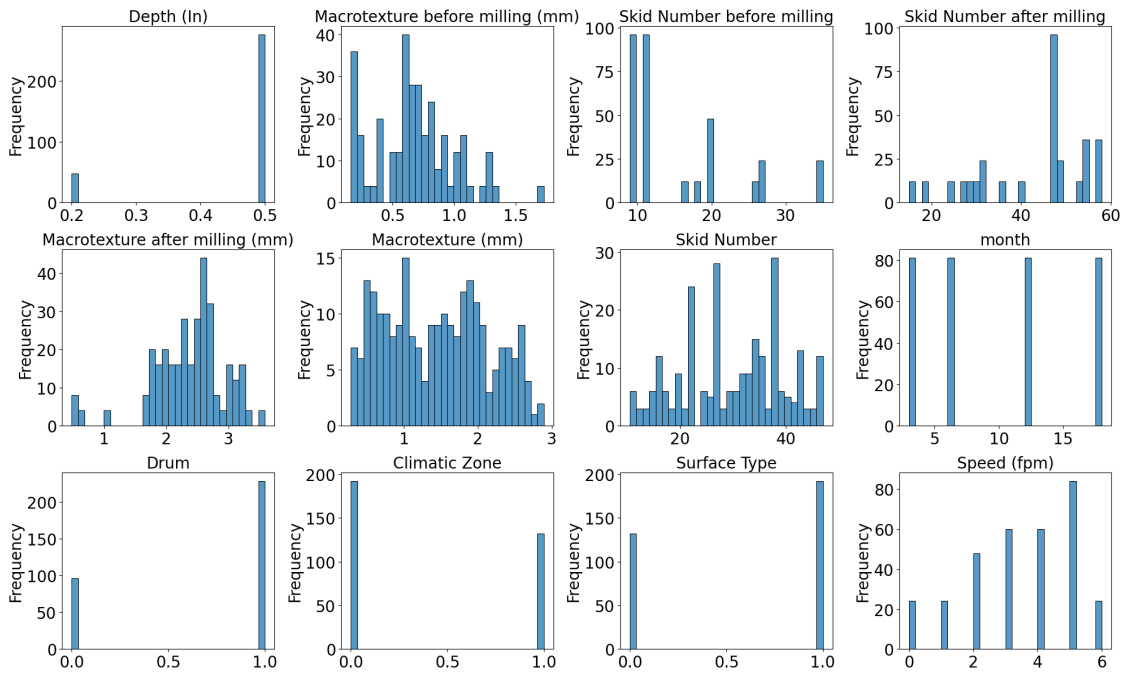


Figure 5: Histogram

Figure 6 illustrates the evolution of skid number following micro-milling treatment on two different surface types: seal coat and HMA. Prior to treatment, both surfaces exhibited relatively low skid resistance—approximately 10 for seal coat and around 25 for HMA. Immediately after micro-milling (at 0 month), both surface types experienced a sharp increase in skid number, rising to about 37 for seal coat and as high as 51 for HMA. This demonstrates the effectiveness of micro-milling in restoring surface friction by increasing surface macrottexture. Notably, the improvement was more significant on HMA surfaces, likely due to their denser aggregate structure and better bonding with

the milling process.

However, starting from the third month, a clear downward trend in skid resistance is observed for both surface types. For seal coat, the skid number dropped rapidly, reaching around 26 at 3 months and declining to below 17 by 12 months, nearly reverting to pre-treatment levels. In contrast, HMA surfaces showed a more gradual reduction and maintained a skid number close to 30 at the 12-month mark. These results suggest that HMA surfaces offer better durability and resistance to polishing, which allows the benefits of micro-milling to persist longer than on seal coat pavements.

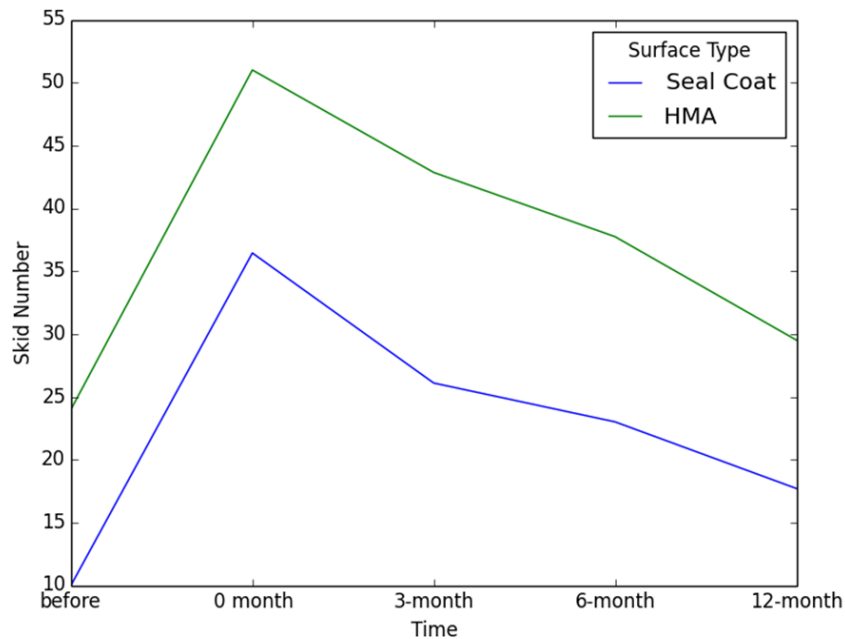


Figure 6: Skid number on different surface type

Figure 7 compares the skid performance of selected sections from three different districts: San Antonio (SAT), San Angelo (SJT), and Abilene (ABL). All districts showed substantial improvement in skid number at 0 month, with SAT and SJT rising to 51 and 46, respectively, while ABL peaked at only 27. From “3 months” onward, district-level differences in deterioration rate became apparent. SAT maintained relatively high skid resistance over time, remaining above 30 at 12 months. In contrast, ABL experienced a rapid decline despite a brief rebound at 6 months, falling back to about 15 by the end of the observation period.

These differences likely reflect the influence of local climate and traffic conditions. For example, SAT may have milder environmental exposure or lower truck traffic volumes, preserving surface

texture for a longer duration. ABL, on the other hand, could be subject to harsher weather or more aggressive traffic loading, which accelerates wear and texture degradation.

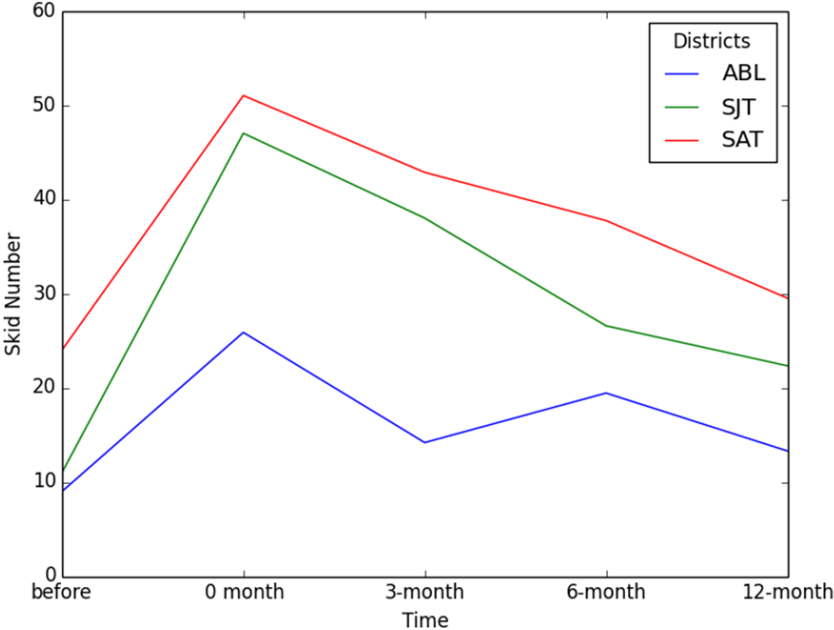


Figure 7: Skid number from different districts

4.3 Modeling Results

This section compares the performance of eight traditional machine-learning baselines with a time series transformer regression Model. The Transformer takes a sliding window of length L (here $L = 4$) and predicts the skid number or macrotexture value at the next inspection month. For fair comparison, all models were evaluated on the same train-test split (80 % / 20 %) and assessed with the coefficient of determination (R^2), root-mean-squared error (RMSE), and mean-absolute error (MAE).

The time series transformer model is implemented in PyTorch and consists of two stacked encoder layers with four self-attention heads and a hidden dimension of 64. Input features at each time step are projected into a 64-dimensional latent space, followed by the addition of learnable positional encodings. The output from the last time step is passed through a two-layer feed-forward network with a hidden size of 32 and ReLU activation to produce a scalar prediction. The model is trained using the Adam optimizer with a learning rate of 10^{-3} and a batch size of 16, using mean squared error as the loss function. Table 2 shows that the Transformer achieves the highest accuracy

for skid-number forecasting ($R^2 = 0.981$), edging out XGBoost ($R^2 = 0.979$) and outperforming all other baselines by a clear margin. Tree-based models (Random Forest, Decision Tree) rank next, whereas linear regressions and the MLP network trail far behind, indicating that non-linear interactions and temporal dependencies are critical for capturing friction degradation.

Table 2: Prediction results for Skid Number.

Model	R^2	RMSE	MAE
Time series transformer	0.981	1.42	0.84
XGBoost	0.979	1.46	0.87
Random Forest	0.967	1.81	1.08
Decision Tree	0.962	1.96	0.82
k-Nearest Neighbors	0.920	2.83	1.35
Ridge Regression	0.776	4.73	3.82
Linear Regression	0.775	4.74	3.88
Lasso Regression	0.726	5.23	4.42
MLP Regressor	0.641	5.99	4.77

The results of the macrotexture prediction are summarized in Table 3. The Random Forest remains the top performer ($R^2 = 0.838$), but the Transformer closely follows with $R^2 = 0.831$ and nearly identical error metrics (RMSE = 0.28; MAE = 0.22). XGBoost ranks third, while linear models again underperform. These findings suggest that, although tree ensembles capture texture variability very well, the Transformer’s sequence modelling adds only marginally more benefit for this target.

Table 3: Prediction results for Macrotexture.

Model	R^2	RMSE	MAE
Random Forest	0.838	0.27	0.22
Time series Transformer	0.831	0.28	0.22
XGBoost	0.809	0.30	0.22
Decision Tree	0.741	0.34	0.27
k-Nearest Neighbors	0.719	0.36	0.29
Ridge Regression	0.686	0.38	0.31
Linear Regression	0.685	0.38	0.31
MLP Regressor	0.646	0.40	0.33
Lasso Regression	0.494	0.48	0.40

Across both targets, ensemble trees (Random Forest, XGBoost) and the Transformer dominate, confirming that non-linear effects, feature interactions, and temporal patterns are essential for accurate forecasting. The Transformer’s slight advantage on skid number demonstrates the value of explicitly modeling sequential dependencies, whereas its comparable performance on macrotexture suggests diminishing returns when historical texture inherently exhibits weaker temporal auto-correlation. These results highlight the practicality of the time series transformer for proactive pavement-management applications, while also showing that well-tuned ensemble methods remain competitive baselines when computational simplicity is desired.

5 Discussion

This study investigated the deterioration of pavement skid resistance and macrotexture following micro-milling treatments, using a sequence-based Transformer model alongside traditional machine learning approaches. The results offer valuable insights into both the behavior of surface characteristics over time and the effectiveness of predictive modeling techniques.

The observed deterioration pattern, initial improvement in skid resistance due to binder removal, followed by a decline from aggregate polishing, and eventual stabilization, is consistent with previous studies. The sharper decline in seal coat sections compared to HMA aligns with findings by Wei et al. [24], who noted that surface type significantly influences the rate of friction loss. The superior durability of HMA surfaces observed in this study may be attributed to their denser aggregate

structure and better resistance to polishing, as also reported by Zhang et al. [32].

The Transformer model outperformed all other models in predicting skid resistance ($R^2 = 0.981$), highlighting the importance of capturing temporal dependencies in pavement performance data. This supports recent advances in deep learning for infrastructure modeling, such as those by Liu et al. [58] and Gao et al. [18], who demonstrated the value of sequence-aware models in predicting long-term pavement behavior. However, for macrotexture prediction, the Random Forest model slightly outperformed the Transformer, suggesting that macrotexture may be more influenced by static or non-temporal factors.

5.0.1 Practical Implications and Limitations

The ability to accurately forecast skid resistance degradation has direct implications for pavement management systems. By leveraging models like the Transformer, transportation agencies can proactively schedule maintenance, prioritize high-risk segments, and optimize resource allocation. Compared to traditional empirical models such as the Penn State or PIARC IFI models, which often lack flexibility and fail to account for environmental variability, the data-driven approach used here offers improved adaptability and predictive power.

Moreover, the inclusion of diverse variables, such as milling depth, drum type, and climatic zone, enhances the generalizability of the model across different operational contexts. This aligns with the recommendations of Koné et al. [51], who emphasized the importance of multi-dimensional input features in improving skid resistance prediction accuracy.

Despite its strengths, the study has several limitations. The dataset, while diverse, is limited in size and temporal scope, covering only up to 18 months post-treatment. This restricts the ability to model long-term deterioration trends or capture seasonal effects. Additionally, the study focused exclusively on micro-milling, limiting the generalizability of the findings to other preventive maintenance methods such as micro-surfacing or fog seals. Variability in construction practices and data quality across districts may also introduce unquantified noise into the models.

5.0.2 Future Research

Future work should aim to expand the dataset both temporally and geographically, incorporating multi-year observations and additional treatment types. Integrating structural indicators and cost data could enable life-cycle cost analysis and optimization, as suggested. Furthermore, the use of high-resolution sensing technologies and in-vehicle data could enhance model inputs and support

real-time pavement condition monitoring. Finally, exploring interpretable AI techniques could help uncover the underlying mechanisms driving surface deterioration and improve stakeholder trust in model outputs.

6 Conclusions

6.1 Summary of Findings

This study systematically evaluated the short- to medium-term effects of milling treatments on pavement skid resistance and macrotexture. A comprehensive dataset from various climatic zones in Texas was used, including 324 samples containing construction parameters, environmental conditions, and time-series surface characteristics. A structured sliding window dataset was constructed to capture the temporal evolution of surface performance after treatment.

The results demonstrated that ensemble models such as XGBoost and Random Forest outperformed conventional methods like linear regression in predicting both skid number and macrotexture. More importantly, the proposed time series transformer-based modeling framework further improved predictive accuracy. Specifically, it achieved the highest $R^2score = 0.980$ for skid number prediction and also ranked second for macrotexture prediction, which validates the effectiveness of modeling surface deterioration as a dynamic sequence prediction task. These findings support the integration of temporal learning techniques into pavement performance modeling, which enables more proactive and data-driven maintenance strategies.

6.2 Limitations

This study focused exclusively on milling as the treatment method and was based on a relatively limited number of field samples with a constrained temporal range. Although the dataset includes a variety of construction, surface, and climate-related variables, it still suffers from data quality inconsistencies, missing values, and unquantified field-level variations such as construction management practices.

In addition, several important factors that influence pavement surface deterioration, including traffic volume, the percentage of heavy vehicles, seasonal variation, and construction timing, were not included in the dataset due to limited data availability. The absence of these variables may introduce bias into the predictive model, especially in relation to traffic loading and environmental conditions. Future studies should consider incorporating these factors to improve model robustness and generalizability.

6.3 Recommendations for Future Work

Several future research areas are recommended. (1) Future studies may incorporate additional preventive treatments such as micro-surfacing or fog seal to compare their long-term impacts on surface friction. (2) Expanding the time horizon to cover multi-year post-treatment performance would enhance the model's practical relevance. (3) Integrating cost data and structural indicators could extend the framework to life-cycle cost analysis and maintenance optimization. (4) Incorporating high-resolution sensing data or in-vehicle measurements could enrich the input space and improve the model's generalizability and real-time applicability.

References

- [1] Yulin He, Chaohe Wang, Xuan Yang, Zepeng Fan, Guoyang Lu, Pengfei Liu, and Dawei Wang. Skid resistance performance analysis and driving safety evaluation in the full life cycle of asphalt pavement. *Journal of Transportation Engineering, Part B: Pavements*, 150(4):04024047, 2024.
- [2] Francesco Canestrari, Eugenio Mariani, and Lorenzo Paolo Ingrassia. Use of wehner-schulze machine to evaluate pavement skid resistance: A review. *Journal of Traffic and Transportation Engineering (English Edition)*, 2024.
- [3] Atul Subedi, Sailesh Acharya, Patrick Singleton, and Michelle Mekker. Safety performance functions and crash modification factors for skid resistance on interstate and non-interstate highways. *Transportation Research Record*, page 03611981251337473, 2025.
- [4] Bradley O Hibbs, Roger M Larson, et al. Tire pavement noise and safety performance, pcc surface texture technical working group. Technical report, United States. Federal Highway Administration. Office of Engineering, 1996.
- [5] Abhinav Kumar and Ankit Gupta. Review of factors controlling skid resistance at tire-pavement interface. *Advances in Civil Engineering*, 2021(1):2733054, 2021.
- [6] Guangwei Yang, Kuan-Ting Chen, Kelvin Wang, Joshua Li, and Yiwen Zou. Field study of asphalt pavement texture and skid resistance under traffic polishing using 0.01 mm 3d images. *Lubricants*, 12(7):256, 2024.
- [7] Eshan V Dave, Jo E Sias, Kaleigh Miech, Rajib B Mallick, et al. Understanding and improving

- pavement milling operations. Technical report, Minnesota. Department of Transportation, 2025.
- [8] Wenbo Li, Mulian Zheng, Zhan Ning, Wenwu Zhang, and Xiaoyan Ding. The design and performance evaluation of low-noise rubber-fibre micro-surfacing pavement. *International Journal of Pavement Engineering*, 25(1):2414056, 2024.
- [9] Mohammad Ali Khasawneh, Ahmad Ali KHASAWNEH, and Tamer ALNAZER. Investigating the impact of pavement surface features on skid resistance: A review on machine learning approach. *Materials Research Proceedings*, 48.
- [10] Song Li, Jinyuan Hu, Yiqiu Tan, Shenqing Xiao, Meizhao Han, Shuai Li, Jilu Li, and Wei Wang. A review of non-contact approach for pavement skid resistance evaluation based on texture. *Tribology International*, page 109737, 2024.
- [11] M-T Do, Malal Kane, Z Tang, and François de Larrard. Physical model for the prediction of pavement polishing. *Wear*, 267(1-4):81–85, 2009.
- [12] Edgar de León Izeppi, Gerardo Flintsch, Samer Katicha, Ross McCarthy, Kevin McGhee, et al. Locked-wheel and sideway-force cfme friction testing equipment comparison and evaluation report. Technical report, United States. Federal Highway Administration, 2019.
- [13] Xiangxi Tian, Yong Xu, Fulu Wei, Oguz Gungor, Zhixin Li, Ce Wang, Shuo Li, and Jie Shan. Pavement macrotexture determination using multi-view smartphone images. *Photogrammetric Engineering & Remote Sensing*, 86(10):643–651, 2020.
- [14] TF Fwa. Pavement skid resistance properties for safe aircraft operations. *Journal of Road Engineering*, 4(4):361–385, 2024.
- [15] José M Pardillo Mayora and Rafael Jurado Piña. An assessment of the skid resistance effect on traffic safety under wet-pavement conditions. *Accident Analysis & Prevention*, 41(4):881–886, 2009.
- [16] Kan Long, Hui Wu, Zhanmin Zhang, Mike Murphy, et al. Quantitative relationship between crash risks and pavement skid resistance. Technical report, Texas. Dept. of Transportation. Research and Technology Implementation Office, 2014.

- [17] James Yichang Tsai, Zhaohua Wang, April Gadsby, et al. Evaluation of the long-term performance and benefit of using an enhanced micro-milling resurfacing method [gdot 13-20]. Technical report, Georgia. Department of Transportation. Office of Performance-Based . . . , 2019.
- [18] Lu Gao, André de Fortier Smit, Jorge A Prozzi, Prasad Buddhavarapu, Mike Murphy, and Linguang Song. Milled pavement texturing to optimize skid improvements. *Construction and Building Materials*, 101:602–610, 2015.
- [19] Robert J Nittinger. Milling and planing of flexible pavement. Technical report, 1977.
- [20] Seonghwan Cho, Oscar Andrés Moncada, Vito Francioso, John E Haddock, et al. Performance-related specifications for pavement milling. Technical report, Purdue University. Joint Transportation Research Program, 2024.
- [21] Bing Hui, Haimei Liang, Shuqi Li, Mu Guo, and Xiaofang Liu. Quality control of micro-milling treatment on tunnel concrete pavement using 3d range data. *International Journal of Pavement Engineering*, 23(5):1612–1621, 2022.
- [22] Shawn S Hung, Arash Rezaei, and John T Harvey. Effects of milling and other repairs on smoothness of overlays on asphalt pavements. *Transportation Research Record*, 2408(1):86–94, 2014.
- [23] Shila Khanal, Amanda Gilliland, Kiran Mohanraj, et al. Ultra-thin bonding wearing course case study. Technical report, United States. Federal Highway Administration. Office of Preconstruction . . . , 2023.
- [24] Jincheng Wei, Zhengchao Zhang, Yulin He, Qianwen Tan, Xiangpeng Yang, Dawei Wang, and Markus Oeser. Study on the skid resistance deterioration behavior of the sma pavement. *Sustainability*, 14(5):2864, 2022.
- [25] Emine Nazan Ünal, Muhammet Komut, and Şenol Altiok. Effect of aggregate and pavement types on skid resistance evolution. *Proc., 7th Eurasphalt and Eurobitume Cong. Madrid, Spain: Kenes Group*, 2021.
- [26] Malal Kane, Michael Lim, Minh Tan Do, and Vikki Edmondson. A new predictive skid resistance model (psrm) for pavement evolution due to texture polishing by traffic. *Construction and Building Materials*, 342:128052, 2022.

- [27] L Chu, B Zhou, and TF Fwa. Directional characteristics of traffic polishing effect on pavement skid resistance. *International Journal of Pavement Engineering*, 23(9):2937–2953, 2022.
- [28] Bo NJ Persson, U Tartaglino, O Albohr, and Erio Tosatti. Rubber friction on wet and dry road surfaces: The sealing effect. *Physical Review B—Condensed Matter and Materials Physics*, 71(3):035428, 2005.
- [29] E Baran. Temperature influence on skid resistance measurement. In *International Surface Friction Conference, 3rd, 2011*, 2011.
- [30] Wenju Peng, Ping Li, Jianping Gao, Zhaohui Liu, Xudong Wang, Shuai Wang, and Wenjie Wu. Long-term skid resistance evolution and influence mechanism of asphalt pavement based on self-developed wear equipment. *Construction and Building Materials*, 453:139085, 2024.
- [31] Yunwei Meng, Zhuochu Chen, Zixiao Wang, Hang Lu, Guangyan Qing, Zhongshuai Liu, and Yanhai Wang. Evaluating the anti-skid performance of asphalt pavements with basalt and limestone composite aggregates: Testing and prediction. *Buildings*, 14(8), 2024. ISSN 2075-5309. doi: 10.3390/buildings14082339. URL <https://www.mdpi.com/2075-5309/14/8/2339>.
- [32] Chen Zhang, Lihao Zeng, Huimin Wang, and Xin Qu. The impact of coarse aggregate mineral compositions on skid resistance performance of asphalt pavement: A comprehensive study. *PloS one*, 19(12):e0308721, 2024.
- [33] Alireza Roshan and Magdy Abdelrahman. Impact of aggregate characteristics on frictional performance of asphalt-based high friction surface treatments. *CivilEng*, 6(1):4, 2025.
- [34] Hongfu Liu, Zi-ang Wang, Chenxi Yang, Siyu Chen, Huanan Yu, Tuo Huang, Xuelian Li, and Zhanping You. Effect of coarse aggregate characteristics on skid resistance deterioration of the ultrathin wearing course. *Journal of Materials in Civil Engineering*, 33(4):04021051, 2021.
- [35] Nabil AlKofahi and Taisir Khedaywi. Evaluation the effect of asphalt film thickness on stripping resistance. *International Journal of Applied Engineering Research*, 14(2):560–570, 2019.
- [36] Ivana Pranjić, Aleksandra Deluka-Tibljaš, Marijana Cuculić, and Robert Skender. Pavement surface macrotexture analysis. In *Proceedings of the 5th International Conference on Road and Rail Infrastructure CETRA*, pages 359–367, 2018.

- [37] Audy Dwi Putra, Sigit Pranowo Hadiwardoyo, and Raden Jachrizal Sumabrata. Skid resistance performance against temperature change of hot-mix recycled asphalt pavement with added crumb rubber. In *AIP conference proceedings*, volume 2114. AIP Publishing, 2019.
- [38] HR Pasindu. Analytical evaluation of impact of groove deterioration on runway frictional performance. *Transportation Research Procedia*, 48:3814–3823, 2020.
- [39] DA Anderson and JJ Henry. Wet-pavement friction of pavement-marking materials. *Transportation research record*, 777:58–62, 1980.
- [40] Yuanfeng Chen, Zhitang Li, Yuankuo Wang, Guoxi Liang, and Xiaolong Yang. A review of long-term skid resistance of asphalt pavement. *Applied Sciences*, 15(4):1895, 2025.
- [41] Abhinav Kumar, Tianchi Tang, Ankit Gupta, and Kumar Anupam. A state-of-the-art review of measurement and modelling of skid resistance: The perspective of developing nation. *Case Studies in Construction Materials*, 18:e02126, 2023.
- [42] Lu Gao, José Pablo Aguiar-Moya, and Zhanmin Zhang. Bayesian analysis of heterogeneity in modeling of pavement fatigue cracking. *Journal of Computing in Civil Engineering*, 26(1):37–43, 2012.
- [43] Adrian Ricardo Archilla and Samer Madanat. Development of a pavement rutting model from experimental data. *Journal of transportation engineering*, 126(4):291–299, 2000.
- [44] Lu Gao, José Pablo Aguiar-Moya, and Zhanmin Zhang. Performance modeling of infrastructure condition data with maintenance intervention. *Transportation research record*, 2225(1):109–116, 2011.
- [45] Zhanmin Zhang and Lu Gao. A nested modelling approach to infrastructure performance characterisation. *International Journal of Pavement Engineering*, 19(2):174–180, 2018.
- [46] Lu Gao, Shi Qiu, and Tejus Renuka Prasad. Bayesian detection of unrecorded maintenance and rehabilitation treatments in pavement management. Technical report, 2017.
- [47] Yuanjiao Hu, Zhaoyun Sun, Yuxi Han, Wei Li, and Lili Pei. Evaluate pavement skid resistance performance based on bayesian-lightgbm using 3d surface macrotexture data. *Materials*, 15(15):5275, 2022.

- [48] TF Fwa. Determination and prediction of pavement skid resistance—connecting research and practice. *Journal of Road Engineering*, 1:43–62, 2021.
- [49] Yuchuan Du, Bohao Qin, Zihang Weng, Difei Wu, and Chenglong Liu. Promoting the pavement skid resistance estimation by extracting tire-contacted texture based on 3d surface data. *Construction and Building Materials*, 307:124729, 2021.
- [50] Jie Ji, Wanyan Ren, Tianhao Jiang, Yuanshuai Dong, Yun Hou, and Haimeng Li. Establishment and analysis of the relationship model between macro-texture and skid resistance performance of asphalt pavement. *Coatings*, 12(10):1464, 2022.
- [51] Aboubakar Koné, Ahmed Es-Sabar, and Minh-Tan Do. Application of machine learning models to the analysis of skid resistance data. *Lubricants*, 11(8):328, 2023.
- [52] Lidan Peng, Lu Gao, Feng Hong, and Jingran Sun. Evaluating pavement deterioration rates due to flooding events using explainable ai. *Buildings*, 15(9):1452, 2025.
- [53] Lu Gao, Ke Yu, and Pan Lu. Considering the spatial structure of the road network in pavement deterioration modeling. *Transportation Research Record*, 2678(5):153–161, 2024.
- [54] Ke Yu and Lu Gao. Pavement missing condition data imputation through collective learning-based graph neural networks. In *International Conference on Transportation and Development 2023*, pages 416–423, 2023.
- [55] Lu Gao, Yao Yu, Yi Hao Ren, and Pan Lu. Detection of pavement maintenance treatments using deep-learning network. *Transportation Research Record*, 2675(9):1434–1443, 2021.
- [56] Farshad Rajabipour, Jinyoung Yoon, et al. Use of machine learning to predict long-term skid resistant of concrete pavement. Technical report, Center for Integrated Asset Management for Multimodal Transportation . . . , 2021.
- [57] Yuhan Weng, Zhaoyun Sun, Huiying Liu, and Yingbin Gu. An interpretable method for asphalt pavement skid resistance performance evaluation under sand-accumulated conditions based on multi-scale fractals. *Sensors*, 25(10):2986, 2025.
- [58] Yang Liu, Zhendong Qian, Haibo Hu, Xijun Shi, and Leilei Chen. Developing a skid resistance prediction model for newly built pavement: Application to a case study of steel bridge deck pavement. *Road Materials and Pavement Design*, 23(10):2334–2352, 2022.

- [59] Lu Gao, Zhe Han, and Yunshen Chen. Deep learning–based pavement performance modeling using multiple distress indicators and road work history. *Journal of Transportation Engineering, Part B: Pavements*, 149(1):04022061, 2023.
- [60] You Zhan, Cheng Liu, Qiangsheng Deng, Qi Feng, Yanjun Qiu, Allen Zhang, and Xianlin He. Integrated fft and xgboost framework to predict pavement skid resistance using automatic 3d texture measurement. *Measurement*, 188:110638, 2022.
- [61] Ashish Vaswani, Noam Shazeer, Niki Parmar, Jakob Uszkoreit, Llion Jones, Aidan N Gomez, Łukasz Kaiser, and Illia Polosukhin. Attention is all you need. *Advances in neural information processing systems*, 30, 2017.
- [62] Qingsong Wen, Tian Zhou, Chaoli Zhang, Weiqi Chen, Ziqing Ma, Junchi Yan, and Liang Sun. Transformers in time series: A survey. *arXiv preprint arXiv:2202.07125*, 2022.
- [63] George Zerveas, Srideepika Jayaraman, Dhaval Patel, Anuradha Bhamidipaty, and Carsten Eickhoff. A transformer-based framework for multivariate time series representation learning. In *Proceedings of the 27th ACM SIGKDD conference on knowledge discovery & data mining*, pages 2114–2124, 2021.
- [64] Shiyang Li, Xiaoyong Jin, Yao Xuan, Xiyu Zhou, Wenhui Chen, Yu-Xiang Wang, and Xifeng Yan. Enhancing the locality and breaking the memory bottleneck of transformer on time series forecasting. *Advances in neural information processing systems*, 32, 2019.
- [65] Yuhong Jin, Lei Hou, and Yushu Chen. A time series transformer based method for the rotating machinery fault diagnosis. *Neurocomputing*, 494:379–395, 2022.
- [66] Kaiming He, Xiangyu Zhang, Shaoqing Ren, and Jian Sun. Deep residual learning for image recognition. In *Proceedings of the IEEE conference on computer vision and pattern recognition*, pages 770–778, 2016.
- [67] Jimmy Lei Ba, Jamie Ryan Kiros, and Geoffrey E Hinton. Layer normalization. *arXiv preprint arXiv:1607.06450*, 2016.
- [68] Ian Goodfellow, Yoshua Bengio, Aaron Courville, and Yoshua Bengio. *Deep learning*, volume 1. MIT press Cambridge, 2016.